A Modular and Interactive OLED-Based Lighting System

Ann Monté, Jurica Kundrata, Jeroen Schram, Maarten Cauwe, Adrijan Baric and Jan Doutreloigne

QUERY SHEET

This page lists questions we have about your paper. The numbers displayed at left can be found in the text of the paper for reference. In addition, please review your paper as a whole for correctness.

Q1: Au: Please confirm all names, affiliations and correspondence for all authors is correct
Q2: Au: References are cited in text as numbers but the reference list is not numbered. Please cite references in text as author/date as per journal style
Q3: Au: Please provide section title
Q4: Au: Please provide location
Q5: Au: Please provide location
Q6: Au: Please provide location/full dates of conference
Q7: Au: Please provide full dates of conference, Doutreloigne et al.
Q8: Au: Please provide up to 10 authors, Friend et al.
Q9: Au: Please provide up to 10 authors, Fry et al.
Q10: Au: Please provide full dates of meeting, Kundrata and Baric
Q11: Au: Please provide up to 10 authors, Lee et al.
Q12: Au: Please provide up to 10 authors/full dates of meeting, Monté et al.
Q13: Au: Please provide up to 10 author names, Villani et al.
Q14: Au: Please provide author/date/page title/date accessed
Q15: Au: Please provide author/date/page title/date accessed

TABLE OF CONTENTS LISTING

The table of contents for the journal will list your paper exactly as it appears below:

A Modular and Interactive OLED-Based Lighting System
Ann Monté, Jurica Kundrata, Jeroen Schram, Maarten Cauwe, Adrijan Baric and Jan Doutreloigne

LEUKOS, 00:1–11, 2017

ISSN: 1550-2724 print / 1550-2716 online
DOI: 10.1080/15502724.2017.1283234

Taylor & Francis
Taylor & Francis Group

A Modular and Interactive OLED-Based Lighting System

Ann Monté[1], Jurica Kundrata[2], Jeroen Schram[3], Maarten Cauwe[1], Adrijan Baric[2], and Jan Doutreloigne[1]
[1]Centre for Microsystems Technology (CMST), IMEC, and Ghent University, Ghent, Belgium
[2]Faculty of Electrical Engineering and Computing, University of Zagreb, Zagreb, Croatia
[3]Holst Centre, Eindhoven, The Netherlands

ABSTRACT The concept of a flexible, large-area, organic light emitting diode (OLED)-based lighting system with a modular structure and built-in intelligent light management is introduced. Such a flexible, thin, portable lighting system with discreetly integrated electronics is important in order to allow the implementation of the lighting system into a variety of places, such as cars and temporary expedition areas. A modular construction of an OLED lighting panel makes it possible to control each OLED cell individually. This not only enables us to counteract aging or degradation effects in the OLED cells but it also allows individual OLED module brightness control to support human or ambient interaction based on integrated or centralized sensors. Moreover, integrating the driving electronics in the backplane of an OLED module improves the energy efficiency of operating large OLED panels. The thin, modular construction and individual, dynamic control are successfully demonstrated.

KEYWORDS aging compensation, flexible, interaction, large-area, lighting system, modular, OLED

1. INTRODUCTION

Current organic light emitting diode (OLED) technology developments are mostly concentrating on material research [1–5], higher efficiency, low-cost production, et cetera. To fully exploit the potential of OLED (foils) in a lighting system, more developments are needed concerning driving electronics, power distribution, integration and miniaturization, human interface, and other added functionality (for example, sensing).

The European FP7 project IMOLA [6] (**I**ntelligent light **M**anagement for **OL**ED on foil **A**pplications) addresses exactly this missing link to a fully flexible lighting product. The main concept of the IMOLA project, illustrated in Fig. 1, is the realization of an interactive, modular, flexible, large-area, OLED-based lighting system on low-cost foil with built-in intelligent light management. The final demonstrator realized within the IMOLA project consists of 15 small panels each containing a 2 × 2 matrix of OLED modules, which is shown in Fig. 2.

Possible applications are widespread, with interesting examples like wall, ceiling, and automotive lighting (both inside and on the outside of the car). The light intensity can be adjusted uniformly on the whole OLED panel, but due to the modular nature the brightness can also be adjusted locally at the module level. This enables advanced

Received 19 July 2016; revised 3 January 2017; accepted 13 January 2017.

Address correspondence to Ann Monté, Centre for Microsystems Technology (CMST), IMEC, and Ghent University, Technologiepark 15, B-9052 Ghent, Belgium. E-mail: ann.monte@imec.be

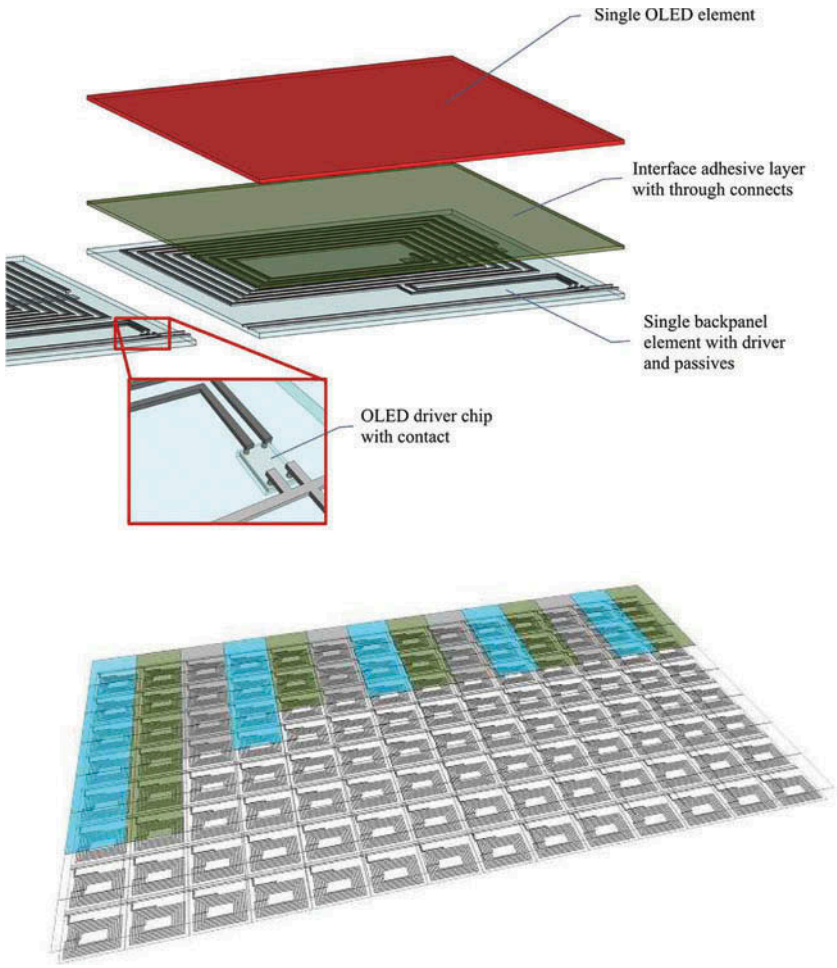

Fig. 1 3D impression of the IMOLA project. The driver and inductor are integrated on the same foil behind each OLED cell.

features with human interaction capability: light on a ceiling or wall can follow the position of a person, or light can gradually move from east to west to create a daylight experience. In case of application in road lighting, light can be adapted depending on the position of a car.

The proposed lighting system is based on state-of-the-art technologies and methodologies; that is, flexible substrates, component embedding, driver design, OLED aging compensation, and gesture sensing. Yet, the combination and integration of all of the different aspects into a flexible, modular, interactive, and lightweight lighting system is far beyond state of the art. Other innovative developments are situated in the OLED driver concept [7] and the technology integration challenges [8].

This article focusses on the OLED driver concept, including OLED aging compensation and human interface, and the challenges imposed by the integration of the electronics. The results are demonstrated in a 2 × 2 matrix of glass OLEDs on a polyethylene terephthalate (PET) substrate making the system semiflexible, but similar results apply onto a fully flexible system with flexible OLEDs. The flexibility of a PET substrate with Cu (copper) tracks is demonstrated in Fig. 3, showing the substrate that was used for driving two OLEDs integrated in the dome of a car. The microcontroller in the middle of the substrate was thinned down to 35 μm in order to improve flexibility.

One could supply the complete OLED panel (consisting of different OLED modules) from one single voltage (OLED modules are driven in parallel) without local voltage control for each individual OLED module. Yet, this has several drawbacks: it is impossible to compensate for individual OLED light output differences; it is very energy inefficient, especially for larger panels, due to the high currents; and human interaction or any other features are not possible. In order to compensate for these drawbacks, the OLED lighting panel is constructed in a modular way, meaning that each OLED is driven by its individual driver chip.

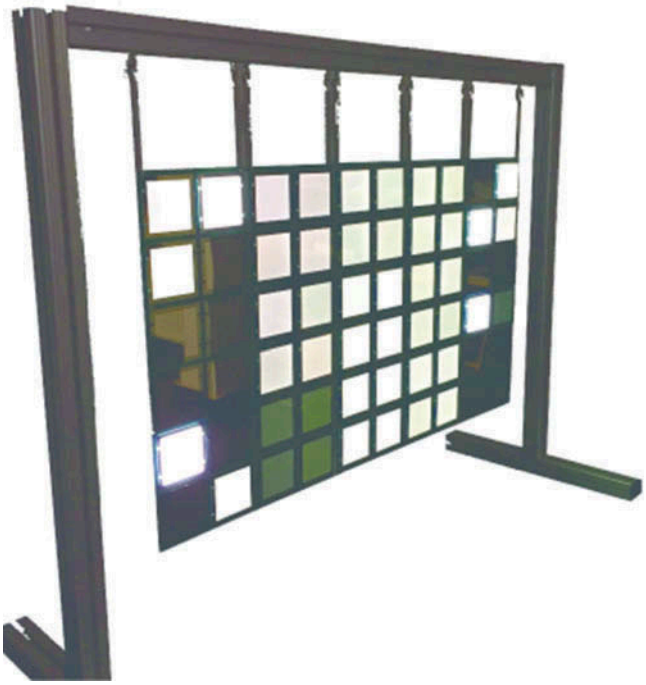

Fig. 2 Final demonstrator of the IMOLA project.

2. OLED DRIVER ELECTRONICS

The concept of the modular construction of an OLED panel has already been demonstrated by Philips' LivingShapes interactive wall [9]. In contrast to the demonstrator we propose in this article, the interactive wall of Philips is very bulky and energy inefficient and does not contain a feedback loop to compensate for individual OLED light output differences.

To meet the demands of the IMOLA project—that is, the maximal integration of the electronics into the backplane of the OLED—a new driver chip was designed. The operation frequency of the driver chip was set high enough in order to allow for a low inductor value (an inductor is needed for the operation of the driver chip; see later) and therefore for a planar inductor.

The OLEDs used in the 2 × 2 demonstrator proposed in this article are the L0023 OLEDs (Mosiled) from Philips. The conversion of the 24 V (lighting standard) to the OLED operating voltage (7.2 V nominal) is done by means of the buck converter integrated on the driver chip. Basically, a buck converter consists of two switches, alternating switching to ground and the supply voltage, and an inductor to stabilize the OLED voltage/current. The voltage conversion is done locally on the backplane of each OLED to avoid high currents in the power supply tracks. Because the goal is to have a thin, unobtrusive, semiflexible system, it is not possible to use an external inductor.

The University of Zagreb did an extensive study on the integration of a planar inductor into the backplane foil [10]. The result is that it is possible to embed inductors with an inductance in the order of 5 to 10 µH. Higher (planar) inductances would occupy a larger area, which is not favorable because the aim is to make a compact system. Moreover, the space allowed for the electronics is limited to the dimensions of the OLEDs, which is about 55 cm^2 for the OLEDs used in the demonstrator proposed in this article. Inductances on the order of 5 to 10 µH are too low for the targeted application in combination with available buck converters. Therefore, a custom-made driver chip was designed that switches at 10 MHz, allowing the integration of a planar inductor into a flexible substrate. In addition to the driving electronics (inductor excluded), the driver chip contains the feedback electronics to control the OLED current [11].

The back and front sides of the 2 × 2 OLED matrix are shown in Figs. 4 and 5. The front side contains both the OLEDs and the sensors for human interaction. The back side contains the inductor coils as well as the four driver chips. Furthermore, a microcontroller can be added in the

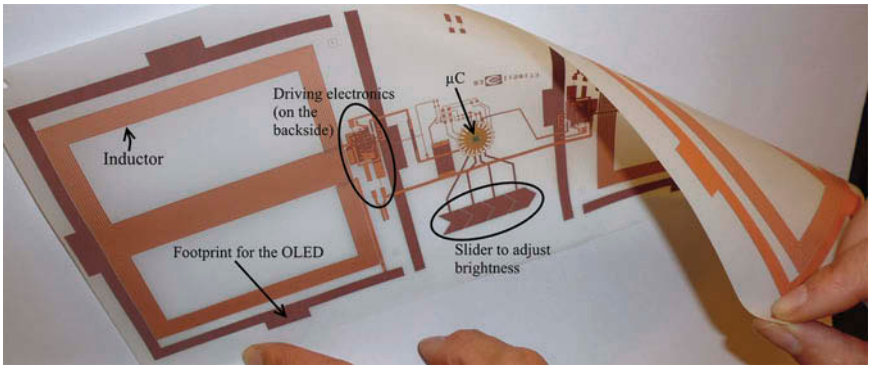

Fig. 3 PET substrate with Cu tracks and a microcontroller.

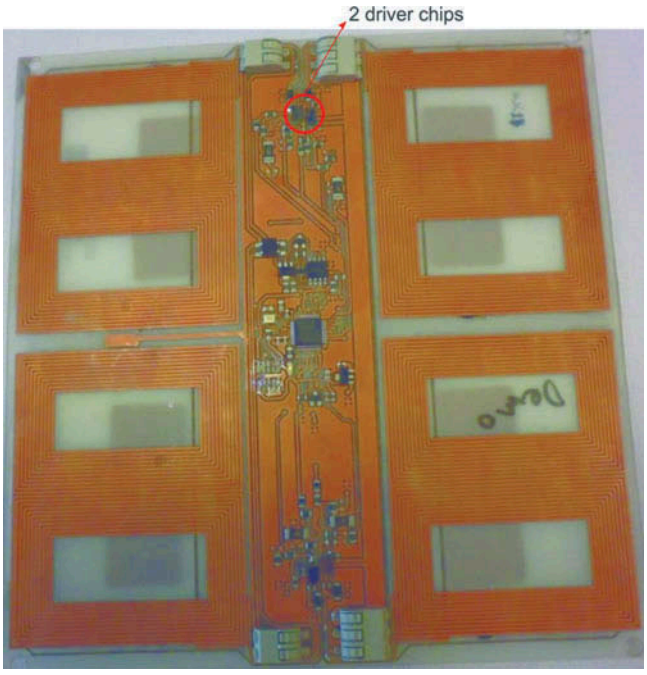

Fig. 4 2 × 2 OLED panel on a 250-µm-thick PET foil—back side. Optionally, a microcontroller can be placed in the middle to add intelligent features such as motion detection.

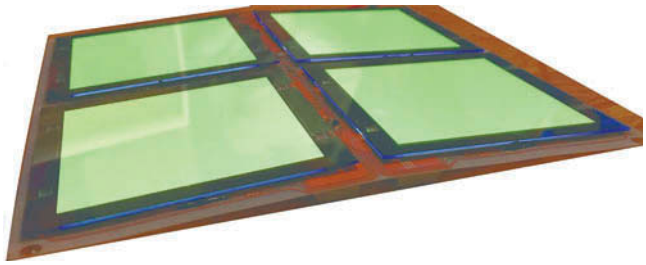

Fig. 5 2 × 2 OLED panel on a 250-µm-thick PET foil—front side.

middle to control the driver chips and to allow (DALI) communication between different OLED panels. The total thickness, excluding the OLEDs and the connectors, is 3.3 mm (in a final application, bulky connectors are not necessary). Choosing thinner off-the-shelf components or thinning down the components as is done with the microcontroller in Fig. 3 allows a theoretical thickness of 320 µm.

In the next sections, the algorithm to compensate for OLED aging, the human interface, and the electrical and optical measurement results are discussed.

3. AGING COMPENSATION

3.1. OLED Aging Modeling

The aging of organic light emitting diodes is more pronounced than in inorganic diodes and it presents a challenge in OLED luminaire design. The aging of an OLED luminaire can be compensated for by applying a smart control algorithm. Ideally the compensation algorithm uses closed-loop control and corrects the luminance degradation based on the feedback from a luminance sensor. Due to the low profile of the OLED luminaire, it is difficult to incorporate a luminance sensor and the compensation algorithm controls the OLED in an open loop. The compensation algorithm increases the driving current of the OLED module as it ages, thus keeping its luminance in a predefined range.

The design of the compensation algorithm is based on the simulation of the OLED module behavior with respect to the time and driving current. The luminous flux of the OLED is proportional to the driving current; that is, the luminance of the OLED is proportional to the density of the driving current [12]. The behavior of the OLED module with respect to the aging process is based on modeling its current efficiency k, which is defined as

$$k = \frac{L}{j}, \tag{1}$$

where L is the luminance and j is the driving current density of the OLED cell. The process of degradation of the OLED is complex and cannot be modeled using a monoexponential decay function. The decay of the current efficiency of the OLED can be accurately modeled using the stretched exponential function [13]

$$k(t) = k_0 \exp\left[-\left(\frac{t}{\tau}\right)^{\beta}\right], \tag{2}$$

where β is the stretch factor, τ is the time constant, and t is the operational time of the OLED. Due to the stretch factor, the relation between the time constant τ and lifetime τ_{70} is

$$\tau_{70} = \tau \sqrt[\beta]{-\ln(0.7)}, \tag{3}$$

where τ_{70} is defined as the time needed for the luminance to decay to 70% of the initial value.

The OLED degrades faster when it is driven by a larger current due to the increased self-heating. This relation between the lifetime τ_{70} and the driving current density j is described by the Coffin-Manson fatigue model [14]

$$\tau_{70}(j) = cj^{-n}, \tag{4}$$

where c is the model constant and n is the aging factor.

The model that relates the luminance of an OLED with its driving current and the operational time is derived by combining the Coffin-Manson model with the stretched exponential functions (2) and (3). This yields the OLED aging model used for simulations of the compensation algorithm

$$k(t_2, j) = k(t_1, j)\exp\left[\ln(0.7)\frac{t_2^{\beta} - t_1^{\beta}}{(cj^{-n})^{\beta}}\right], \qquad (5)$$

where $k(t_1, j)$ is the current efficiency at the beginning, and $k(t_2, j)$ is the current efficiency at the end of the simulated period at a given driving current density. The model assumes that the efficiency ages for a given time period and a given current level in the same manner independent of the driving current levels in the previous time periods. Table 1 shows the model parameters that are fitted using the measurement data at room temperature (T = 25°C). The data are based on measuring the OLED output luminance as it degrades with time for four different levels of the driving current density and consists of three measurements per current density level; that is, a total of 12 measurements.

3.2. Compensation Algorithm Design

The goal of the compensation algorithm is to increase the lifetime τ_{70} of an OLED luminaire beyond the nominal lifetime of the OLED module. The studied compensation algorithm consists of two driving current increments ΔI_1 and ΔI_2 introduced after the time periods ΔT_1 and ΔT_2. The number of algorithm parameters is reduced by fixing the second current increment to a defined maximum current level I_{limit}. Figure 6 shows an example algorithm design.

The figures of merit of the algorithm design simulations are the lifetime τ_{70} and the luminance error ε_L. The luminance error is the root mean square error of the luminance with respect to the initial nominal luminance L_0. The compensation algorithm is analyzed using the numerical simulations of the OLED module

TABLE 1 Parameters of the OLED cell and its aging model

Parameter name	Parameter value
Nominal luminance L_0	2000 cd/m^2
Nominal current I_0	300 mA
Nominal current density j_0	8 mA/cm^2
Nominal lifetime τ_{70}	10 kh
Stretch factor β	0.818
Ageing factor n	2.14
Constant c	1.46e5 h * (A/m^2)^n

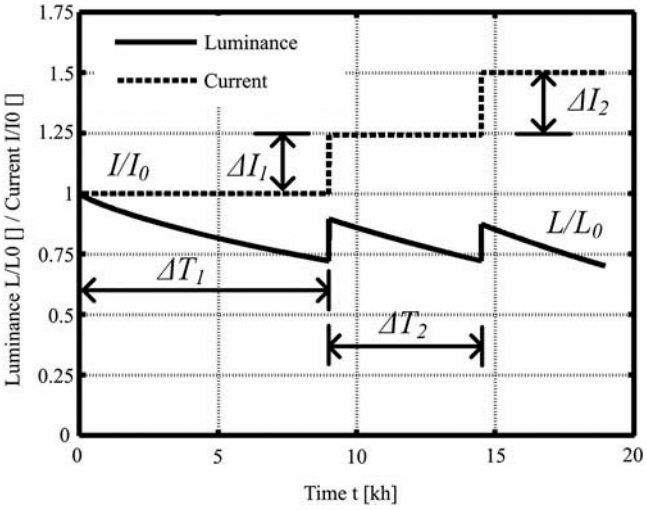

Fig. 6 Example algorithm design with Pareto-optimal parameters (ΔI_1 = 24% I_0, ΔI_2 = 26% I_0, ΔT_1 = 9 kh, ΔI_2 = 5.5 kh).

by varying the parameters of the compensation algorithm. The simulations of the OLED module and the compensation algorithm are based on the parameter sweeps in Table 2.

Figure 7 shows the simulation results in the lifetime-luminance error space where the Pareto front is emphasized. The Pareto front designs maximize the lifetime while minimizing the luminance error of the OLED luminaire. Table 3 shows the parameters of Pareto-optimal designs I, II, and III in Fig. 7.

The simulation results show that the lifetime τ_{70} ranges from 16,000 to 19,000 h, which is a 60% to 90% increase from the nominal lifetime. The luminance root mean square error ranges from 280 to 400 cd/m^2, which is 14%–20% of the nominal luminance. The results also show that there is a trade-off between the lifetime increase and the luminance error; that is, the algorithm that greatly increases the lifetime also causes larger deviations of the OLED luminance from its nominal value. The three examples of Pareto-optimal design show that an increase of the current increment ΔI_1 increases both the lifetime τ_{70} and luminance error ε_L, while the time period ΔT_2 remains the same.

TABLE 2 Simulated parameters of the compensation algorithm

Parameter name	Parameter value
Current increment ΔI_1	0–50%
Current limit I_{limit}	1.5 I_0
Time period ΔI_1	5–10 kh
Time period ΔI_2	0–10 kh

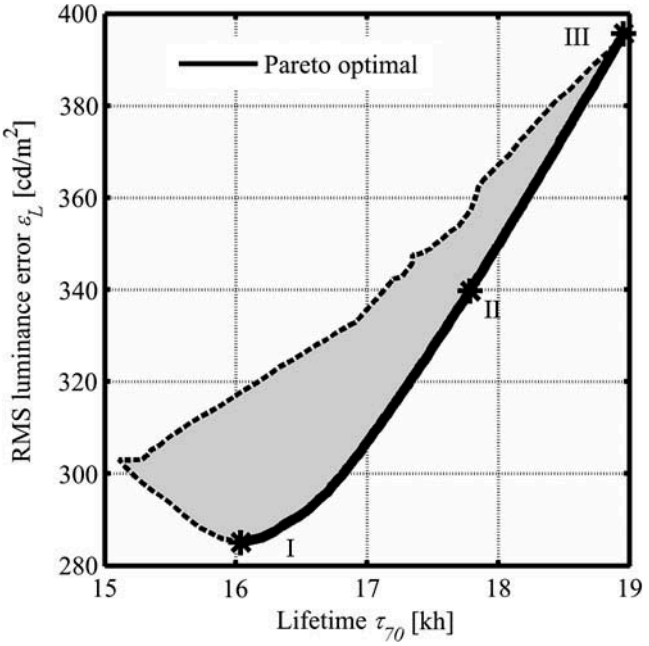

Fig. 7 **Results of the algorithm simulation in the RMS luminance error versus lifetime space and the front of the Pareto-optimal algorithm designs.**

TABLE 3 **Example Pareto-optimal designs of the compensation algorithm**

Design no.	τ_{70} (kh)	ε_L (cd/m^2)	$\Delta I_1/I_0$ (%)
I	16	285	16.5
II	18	340	21.6
III	19	396	34.5
Design no.	**$\Delta I_2/I_0$ (%)**	**ΔT_1 (kh)**	**ΔT_2 (kh)**
I	33.5	6.58	5.02
II	28.4	7.11	4.99
III	15.5	8.42	4.98

The parameters of the compensation algorithm are determined using the OLED aging model. The algorithm uses open-loop control of the driving OLED current and thus it is implemented in the backplane firmware of the OLED luminaire using a single function. The main purpose of the function is to keep track of the operational time t of the OLED module and to update the driving current according to the compensation algorithm.

The compensation algorithm uses two current increments and can be improved by adding additional current increments. By breaking the current adjustment into more than two discrete current increments, a lower luminance error could be achieved. Using more current increments also requires a more accurate model of the OLED aging because the error of the OLED aging model is accumulated during the execution of the algorithm at each current increase. The compensation algorithm offsets the reduced current efficiency due to OLED aging by increasing the driving current. This in turn also increases the power consumption of the luminaire and decreases its efficiency. Though the increased driving current compensates for the luminance decay, it also accelerates the changes in the spectrum composition of the OLED cell. The resulting algorithms are not experimentally verified due to the long duration of such measurements (up to 20,000 hours). Potential inaccuracies of the luminance aging model can result in a shorter lifetime of the luminaire than predicted (caused by incorrect parameters of the aging compensation algorithm) or a greater variability of its luminance during operation.

4. HUMAN INTERFACE

Ordinary lighting fixtures are getting more functions, such as the possibility of controlling them with a smartphone in a Domotica system, based on DMX, Zigbee, DALI, or other protocols. Regardless of these external controls, simple, direct control over lighting is still desirable. To account for this, a human interface was implemented in the backplane of the OLED panel (consisting of a 2 × 2 matrix of OLED modules; Fig. 5), allowing the user to have direct control over the light output of the lighting module without the need for an external controlling device.

The human interface that is developed consists of both a gesture sensor and a sound detector. The gesture sensor can be used to control an individual backplane and to accurately control the light output from the OLED panel, whereas the sound detector can be used for quick on–off interaction and interact with multiple panels simultaneously. Figure 8 shows where the electronics of the OLED panel are located.

4.1. Gesture Sensing

The gesture sensor consists of an optical sensor (si1443 from Silicon Labs) combined with three infrared LEDs, placed at a distance of 55 mm on three sides of the sensor. The infrared (IR) LEDs are each driven sequentially after each other by the sensor multiple times per second. After driving an IR LED, the amount of reflected infrared light is measured. When the measurement is complete, the sensor drives the second IR LED, et cetera.

Combining the reflective measurement data and comparing this to a threshold, the presence of an object in front of the sensor can be detected. Because the

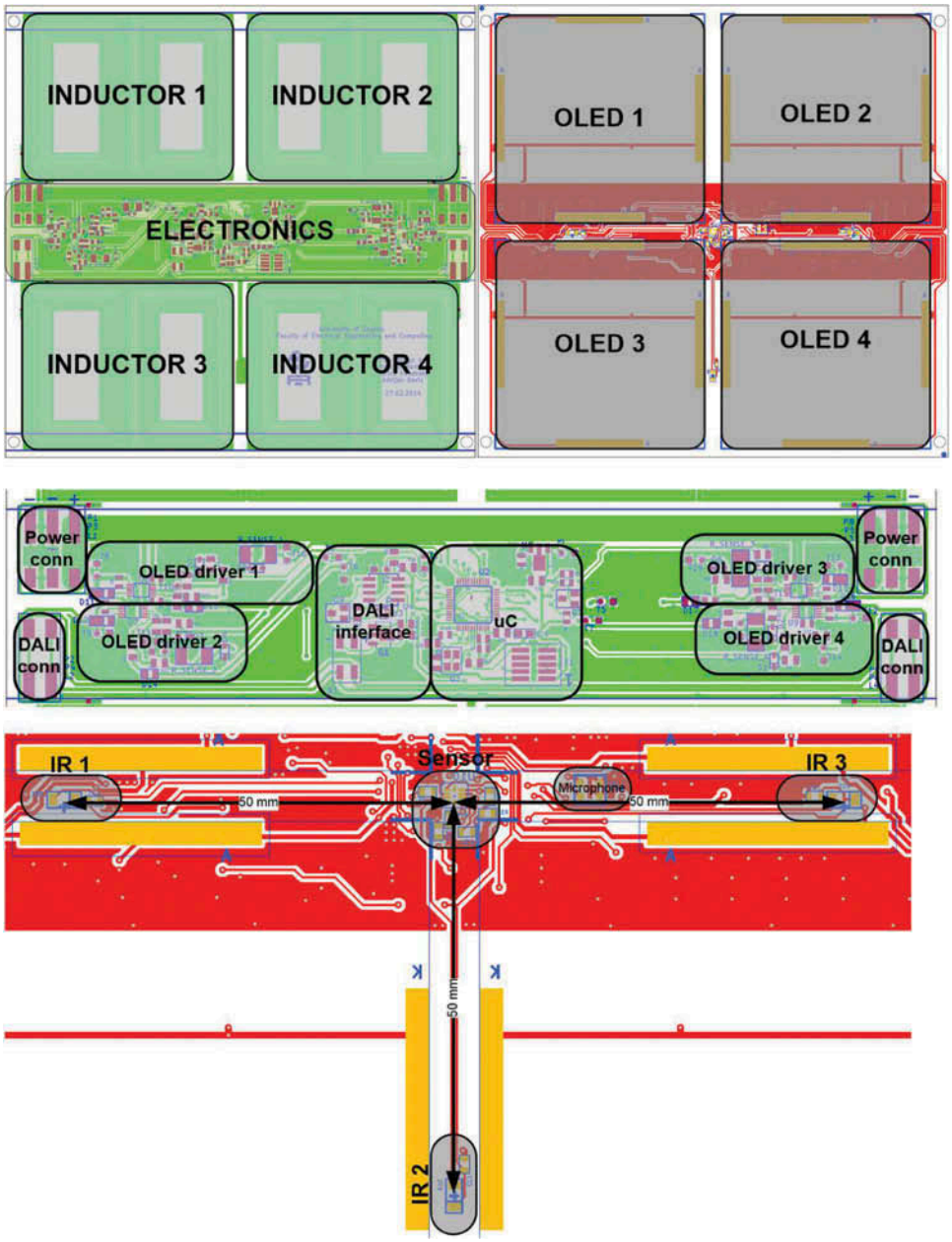

Fig. 8 Human interface: gesture sensing and sound detection.

measurement will take place multiple times per second, changes in the reflected infrared light can be observed. By looking at the location of the peaks in the measured channels in time, several preprogrammed gestures can be recognized. Storage and analysis of the measurement data is done in the firmware of the microprocessor that drives the intelligent backplane.

Plots of the measured data with this sensor with different hand gestures are provided in Fig. 9.

After determining the hand gesture, the four OLEDs on the backplane are driven correspondingly. Functions such as increasing and decreasing the light intensity with up and down hand gestures were implemented into the final demonstrator as well as the ability to select an individual OLED by waving left and right. Such gesture sensing interface could be implemented in the dome light of a car, selecting the driver or passenger side and tuning the light intensity without compromising a clean look of the interior. For a wall lighting application, the gesture sensing can be used to realize an interactive showpiece as seen in Fig. 2. By waving gestures in front of the wall light, a user is able to "draw" patterns in order to realize a dynamic lighting canvas.

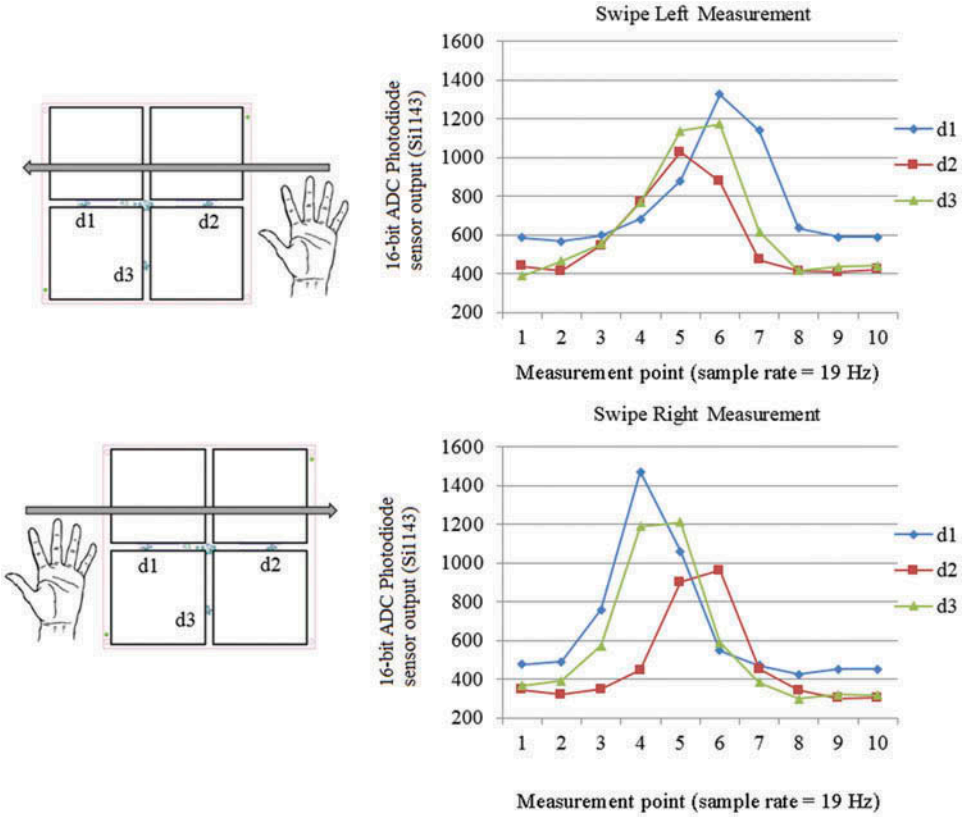

Fig. 9 Raw sensor measurements data—left swipe and right swipe gestures.

4.2. Sound Detection

Because the gesture-based sensors will allow interaction with each individual backplane or even individual OLEDs, it was decided that sound detection would be used for interaction with a larger setup, consisting of multiple backplanes, as a single entity. However, because a backplane should also be able to function by itself, a microphone should be implemented in each individual backplane.

For sound sensing, it was determined that only a reaction of the system to a peak sound—for example, a hand clap or another loud, short sound—was needed. The idea behind this is to have the system respond to a clap to be turned on or off completely, as in the well-known "Clapper" light switch.

Because of this, a simple amplifier circuit connected to a microphone component was sufficient to act as a high-level interrupt input for the microprocessor when a sound peak was present. Regardless of hand gestures, all backplanes, whether by themselves or in a grid, will turn all OLEDs on if a clap is made by the person interacting with the installation. Another clap will dim all of the OLEDs. If separate tiles were placed in a room without a data connection between them, the sound detection would allow the user to easily switch on or off all OLED panels at once by clapping his hands.

When the human interface in the wall light demonstrator is not detecting any gestures or claps for a set amount of time, the intelligent backplane switches to idle mode, where there is a soft "breathing" pattern presented on the OLEDs. The backplane will then remain in this mode until an interaction is detected or the system is reset.

5. MEASUREMENT RESULTS

The size of the proposed 2 × 2 OLED matrix is 16 cm × 16 cm with a thickness of 3.3 mm. The efficiency of this 2 × 2 OLED matrix is shown in Fig. 10 and is calculated as the total power dissipated in the four OLEDs and their feedback resistor divided by the power generated by the 24-V supply.

The highest efficiency occurs when the OLEDs generate their maximum power. The total power dissipated by the communication and control electronics (thus excluding the power dissipated by the driver chip) is 580 mW.

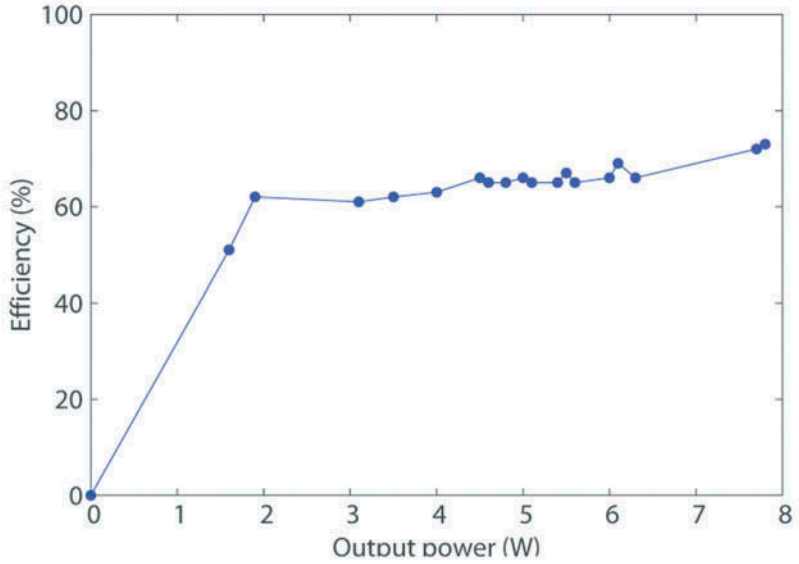

Fig. 10 Efficiency of the 2 × 2 OLED panel.

Without the communication and control electronics, the efficiency would be about 75% for an output power higher than 2 W.

Compared to state-of-the-art (O)LED drivers, efficiencies of about 70% seem quite low at first. Peak power efficiencies of 96% are reported for a chain of multiple series-connected LEDs attached to the output of the driver. Yet, when driving a single LED at 1 A output current, this value drops to about 85%. Moreover, these power efficiencies are obtained by using a very large (50–100 μH), almost ideal external inductor, specifically designed for high-current applications with a parasitic series resistance of only 100 mΩ. Because the goal of IMOLA is a (semi-)flexible system with maximal integrated electronics, the use of such a (bulky) inductor is not possible. Yet, when targeting an application in which there are no strong limitations regarding the thickness of the backplane, discreet inductors can be used resulting in a slightly higher efficiency.

The optical performance is mainly determined by the type of OLEDs used; that is, the L0023 OLEDs (Mosiled) from Philips in this demonstrator. According to the datasheet, the luminous flux is 27.5 lm and the luminance is 2000 cd/m^2 at the nominal current (270 mA). For lighting applications such as the wall light in Fig. 2, consisting of several OLEDs next to each other, it is very important to know the luminance uniformity between the different OLEDs. Figure 11 shows the spectrum of the four OLEDs driven at 250 mA at the same time. The maximum difference that occurs between a point on one of the spectra and its corresponding average point is 2.5 mW/sr/m^2, which is very close to the margin of measurement error. The different spectra seen from different angles are shown in Fig. 12. Indeed, the light output changes with the angle at which the OLED is observed. This is illustrated once more in Table 4, showing the luminance, color temperature, and chromaticity components u' and v' as a function of the angle to the surface normal.

At 250 mA the luminous flux of one OLED is about 25.5 lm and the power generated by the power supply is 10.7 W, resulting in a luminous efficacy of about 9.5 lm/W for the total system.

6. CONCLUSION

The concept of a flexible, large-area, OLED-based lighting system with a modular structure, discreetly integrated electronics, and built-in intelligent light management has been introduced. Such a flexible, lightweight OLED lighting system is very important to allow its introduction in a broad market. The modular construction of an OLED lighting panel makes it possible to control each OLED cell individually, allowing aging or degradation compensation in individual OLED cells as well as OLED brightness control to support human or ambient interaction.

FUNDING

This work was supported by the European Commission under the 7th Framework Programme through the IMOLA project (GA 288377). The sponsors did not

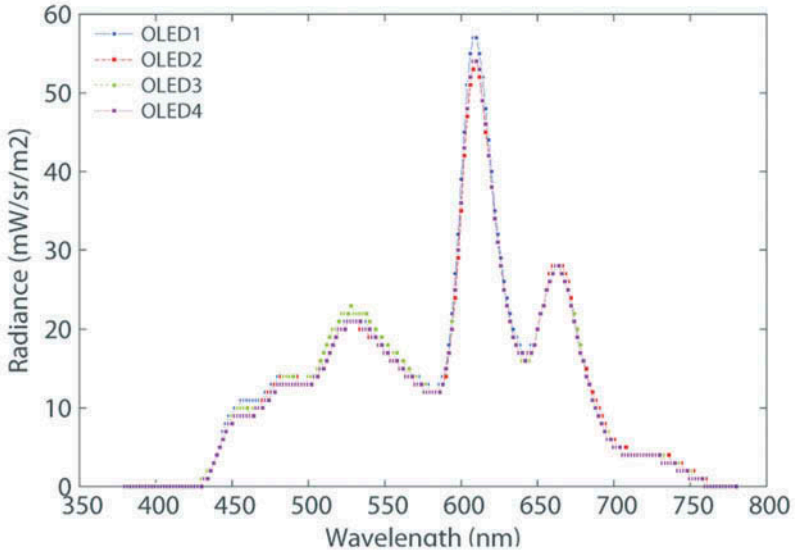

Fig. 11 Spectrum of the four OLEDs on the 2 × 2 OLED panel (OLED current = 250 mA).

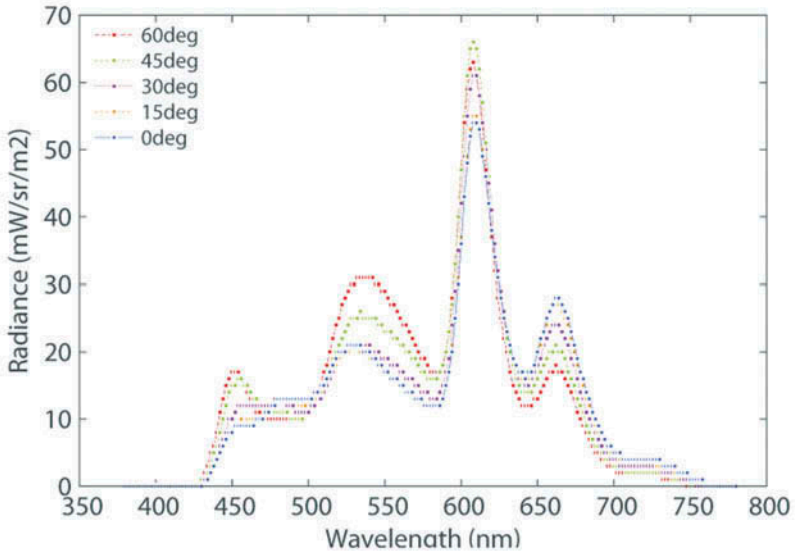

Fig. 12 Spectrum as a function of the angle to the surface normal (OLED current = 250 mA).

TABLE 4 Light output as a function of the angle to the surface normal (OLED current = 250 mA)

Angle (°)	L (cd/m^2)	CCT (K)	u'	v'
60	1954	3428	0.234	0.524
45	1806	3010	0.250	0.521
30	1603	2824	0.258	0.521
15	1494	2873	0.256	0.523
0	1498	2900	0.254	0.523

have any role in the design, experiments, and article writing. The authors declare that there is no conflict of interest.

REFERENCES

Cauwe M, Sridhar A, Sterken T. 2014. Technology development for a flexible, low-cost backplane for lighting applications. In: IMAPS Benelux Spring Event: Packaging for Lighting and Photonics.

Doutreloigne J, Monté A, Windels J. 2013. Design of an integrated OLED driver for a modular large-area lighting system. In: Proceedings of the 7th International Conference on Circuits, Systems and Signals; Cambridge, MA.

Forrest SR. 2003. The road to high efficiency organic light emitting devices. Org Electron. 4:45–48.

Friend RH, and others. 1999. Electroluminescence in conjugated polymer. Nature. 397:121–128.

Fry C, and others. 2005. Physical mechanism responsible for the stretched exponential decay behavior of aging organic light-emitting diodes. Appl Phys Lett. 87:213502. <http://www.architonic.com/pmsht/living shapes-interactivewall-philips-lumiblade-oled/1201916≥

Hung LS, Chen CH. 2002. Recent progress of molecular organic electroluminescent materials and devices. Mater Sci Eng. 39:143–222. <http://www.imola-project.eu/≥
Kundrata J, Baric A. 2012. Design of a planar inductor for DC-DC converter on flexible foil applications. In: Proceedings of the 35th International Convention MIPRO2012; Opatija, Croatia.
Lee KC, and others. 2001. Application of the stretched exponential function to fluorescence lifetime imaging. Biophys J. 81(3):1265–1274.
Monté A, and others. 2013. Driving electronics for OLED lighting. In: SID Mid-Europe Spring Meeting; Ghent, Belgium.
Tang CW, VanSlyke SA. 1987. Organic electroluminescent diodes. Appl Phys Lett. 51:913–915.
Villani F, and others. 2009. Inkjet printed polymer layer on flexible substrate for OLED applications. J Phys Chem C. 113(30):13398–13402.
Wang H, Klubek KP, Tang CW. 2008. Current efficiency in organic light-emitting diodes with a hole-injection layer. Appl Phys Lett. 93 (9):093306.

AUTHOR BIOS

Ann Monté was born in Zottegem, Belgium, in 1980. She received the M.Sc. and Ph.D. degrees in electronics engineering from the University of Ghent, Belgium, in 2003 and 2008, respectively. She is affiliated with the Inter-University Microelectronics Centre (IMEC), in the CMST group at the University of Ghent. She is involved in research on the design of driver electronics for both displays and lighting. She is author or coauthor of 20 papers in international technical journals and conference proceedings.

Jurica Kundrata (S10) received his master's degree in electronics engineering and information technology from the University of Zagreb Faculty of Electrical Engineering and Computing (UNIZG-FER) in 2011. Currently, he is pursuing his Ph.D. degree from the University of Zagreb. His research interests include multiphysics simulation, electromagnetic compatibility, and design of magnetic passives and their application in DC-DC converters.

Jeroen Schram works as electrical engineer at the Holst Centre where he is responsible for the electrical and circuit design of embedded printed electronics applications in the Systems in Foil department. He holds a bachelor's degree in electrical engineering from the Fontys University of Applied Science in Eindhoven (2010). From 2010 to 2011 he worke at Bruns BV, designing and developing control systems for interactive exhibitions. He has been working at Holst Centre since 2011.

Maarten Cauwe (M) received a master's degree in electronics engineering from Ghent University, Ghent, Belgium, and a Ph.D. from the Center for Microsystems Technology (CMST), a joint research lab of IMEC and Ghent University. He is currently leading the Advanced Packaging Team at CMST and is involved in several projects concerning substrate technologies, chip assembly, advanced interconnection, and chip embedding. His previous research work was focused on component embedding in printed circuit boards. He is currently coordinating a project on this topic in cooperation with the European Space Agency.

Adrijan Baric (M98) received Dipl.-Ing. and M.Sc. degrees in electrical engineering from the University of Zagreb, Zagreb, Croatia, in 1982 and 1985, respectively, and a Ph.D. in electronics from the Dublin City University, Dublin, Ireland, in 1995. Since 1984, he has been with the University of Zagreb, where he is currently a professor. His research interests include semiconductor device modeling, integrated circuit design, interconnect modeling, and electromagnetic compatibility.

Jan Doutreloigne received M.Sc. and Ph.D. degrees in electronics engineering from the University of Ghent, Belgium, in 1987 and 1992, respectively. From 1992 to 1998 he was a full-time lecturer at the University of Cuenca, Ecuador, in the area of electronics, telecommunications, and computer sciences. In 1998, he joined the Inter-University Microelectronics Centre (IMEC), in the Centre for Microsystems Technology (CMST) research group at the University of Ghent, where he is in charge of the full-custom design of mixed analog–digital driver ASICs for high-voltage display and telecom applications. He is currently also a professor at the same university.